Electronic Supplementary Material (ESI) for Dalton Transactions

Ligand-based Molecular Recognition and Dioxygen Splitting: An Endo Epoxide Ending

*Peter E. Sues, Matthew W. Forbes, Alan J. Lough, and Robert H. Morris**

Department of Chemistry, University of Toronto, Toronto, Ontario M5S 3H6, Canada

Table of Contents:

Table S1. Selected Bond Lengths (Å) and Angles (deg) for 2 and 5.

	2	**5**
	Bond Lengths (Å)	
Ru(1)-P(1)	2.279(2)	2.331(4)
Ru(1)-P(2)	2.299(2)	2.277(4)
Ru(1)-P(3)	2.377(2)	2.376(4)
C(1)-C(2)	1.473(9)	1.32(2)
	Bond angles (deg)	
P(1)-Ru(1)-P(2)	83.55(6)	81.9(2)
P(1)-Ru(1)-P(3)	100.64(6)	89.9(2)
P(2)-Ru(1)-P(3)	91.01(6)	89.4(2)

Table S2. Selected Crystal Data, Data Collection, and Refinement Parameters for Compounds 2 and 5.

	2	**5**
empirical formula	$C_{48}H_{47}O_2P_3Ru$	$C_{48}H_{47}P_3RuS$
FW	849.84	949.90
lattice type	monoclinic	triclinic
space group	C2/c	P-1
T, K	150(2)	147(2)
a, Å	22.139(4)	10.691(1)
b, Å	11.663 (2)	12.001(2)
c, Å	33.324(6)	19.006(2)
α, deg	90	73.029(9)
β, deg	104.066(6)	88.592(9)
γ, deg	90	70.042(9)
V, Å^3	8347(3)	2184.8(4)
Z	8	2
ρ_{calc}/Mg m^{-3}	1.353	1.292
μ(Cu, Kα) mm^{-1}	0.529	4.619
F(000)	3520	880
cryst size, mm^3	0.28 x 0.20 x 0.20	0.03 x 0.02 x 0.02
range θ collected, deg	1.90 to 27.52	4.10 to 66.74
reflns collected/unique	20144/9529	43998/7367
abs cor	Semi-empirical from equivalents	
Max and min transmn coeff.	0.7456 and 0.7122	0.7528 and 0.6458
goodness of fit	1.040	1.147
R_1(I>2σ(I))[a]	0.0350	0.0556
wR_2 (all data)[a]	0.0800	0.1713
peak and hole, e Å^{-3}	0.376 and -0.417	1.274 and -2.671

[a] Definition of R indices: $R_1 = \Sigma(F_O - F_C)/\Sigma(F_O)$; $wR_2 = [\Sigma[w(F_O^2 - F_C^2)^2]/[\Sigma[w(F_O^2)^2]]]^{1/2}$

VT NMR Discussion

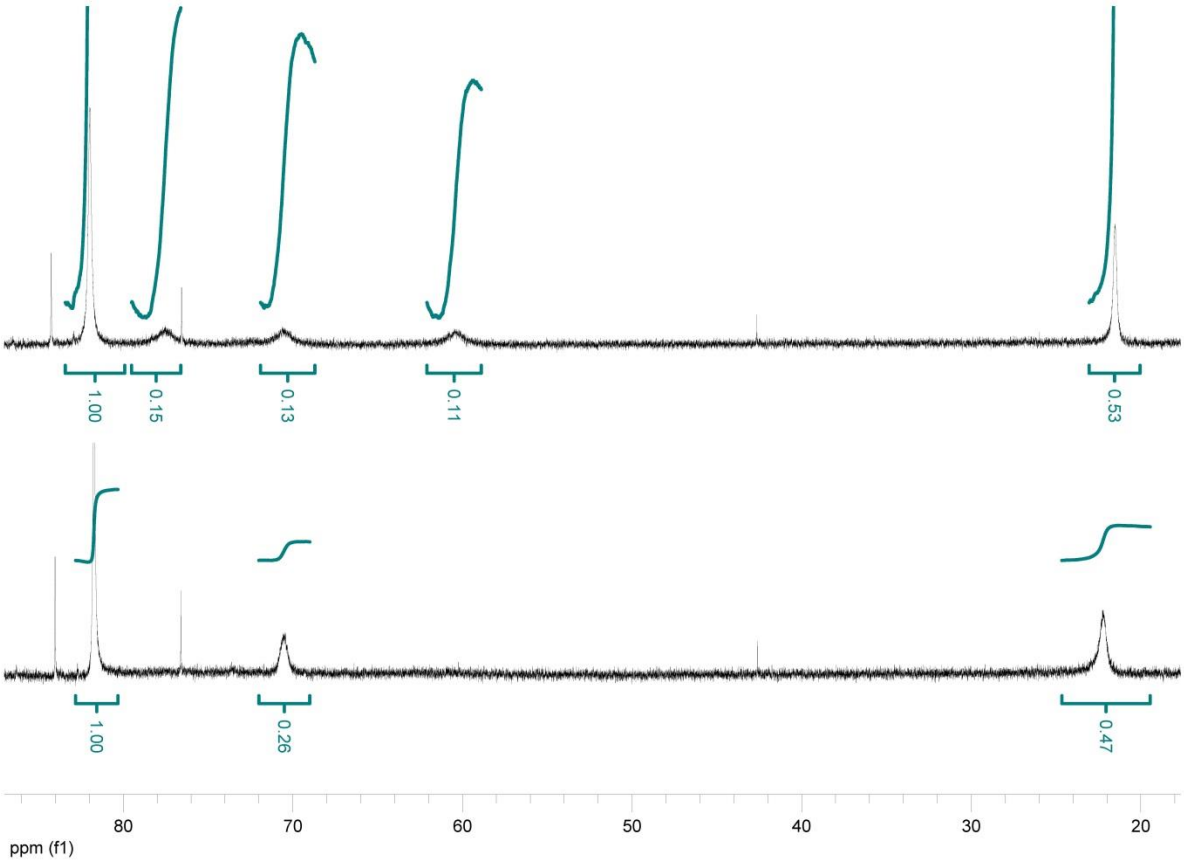

Figure S1. Variable temperature ^{31}P {^{1}H} NMR (THF-d_8) spectra of the oxygen activation reaction mixture. The top spectrum was taken at a temperature of -80°C, while bottom spectrum was taken at a temperature of -60°C.

In the spectrum taken at -80°C the starting material can be seen at 82 and 22 ppm, the product epoxide can be seen around 71 ppm (the peaks for the phosphoryl and dppen ligands overlap), and the peroxo-intermediate can be seen at 78 and 60 ppm. Upon heating to -60°C the peroxo-intermediate disappeared, and the integration value for the product increased in a roughly proportional amount to the disappearance of the intermediate species (it should be noted ^{31}P NMR integrations are not qualitative, and this is purely a qualitative observation)..

Electrochemical Discussion

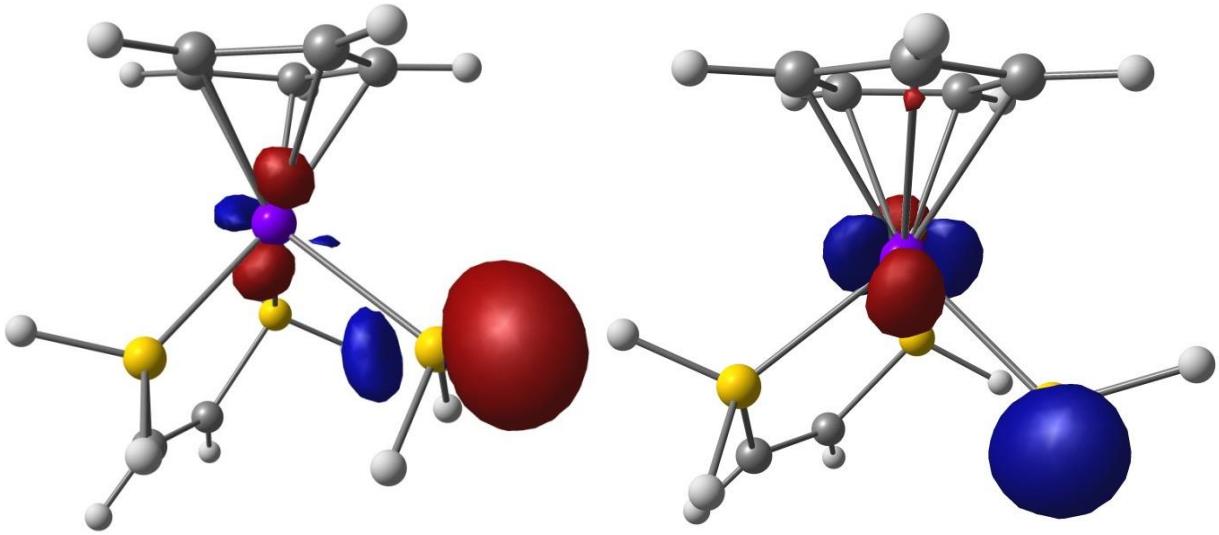

Figure S2. Pictorial representations of the HOMO (left) and SOMO (right) for **A** and **B**, respectively.

We have assigned the two quasi-reversible redox couples that were detected with an E_{pa} and E_{pc} of 0.51V and 0.25V, as well as -0.48V and -0.73V vs. SCE, as metal- and ligand-based, respectively, based on the molecular orbitals of **A** and **B** generated by our computational studies (Figures 4 and S1). The HOMO of **A** has a significant ligand-based contribution, while the SOMO of **B** has more metal character, and as such we view the first oxidation of **1** as removal of a phosphido electron and the second oxidation as removal of a d-electron.

Cartesian Coordinates and Free Energies of Optimized Structures.

O_2

$G°_{solv}$ -94290.6391018

O	0.00000	0.00000	0.60313
O	0.00000	0.00000	-0.60313

A

$G°_{solv}$ -874230.6690071

Ru	-0.37586	0.00508	0.00004
P	1.27557	-0.39720	1.50312
P	1.27546	-0.39784	-1.50297
P	0.33017	2.31481	-0.00046
C	2.89112	-0.65529	-0.66679
H	3.79917	-0.80031	-1.25288
C	2.89117	-0.65495	0.66689
H	3.79928	-0.79968	1.25298
C	-2.44950	0.48460	0.71625
C	-2.11183	-0.83106	1.14944
C	-1.92112	-1.65815	0.00032
C	-2.11178	-0.83152	-1.14914
C	-2.44943	0.48432	-0.71649
H	1.32361	2.43483	1.02999
H	1.32366	2.43443	-1.03087
H	1.64938	0.55617	2.48731
H	1.64920	0.55515	-2.48755
H	1.22739	-1.53107	-2.35529
H	-2.03234	-1.15537	-2.18164
H	-2.67609	1.33008	-1.35569
H	-2.67617	1.33062	1.35510
H	-2.03248	-1.15451	2.18207
H	-1.69429	-2.71778	0.00053
H	1.22765	-1.53011	2.35587

O_2^-

$G°_{solv}$ -94358.5043675

O	0.00000	0.00000	0.66395
O	0.00000	0.00000	-0.66395

B

$G°_{solv}$ -874128.0686235

Ru	0.37398	0.06376	-0.08675
P	-1.35444	-0.91399	-1.29313
P	-1.27758	0.29824	1.49086
P	-0.10882	2.18675	-0.79752
C	-2.88878	-0.29195	0.86167
H	-3.77638	-0.20397	1.48792
C	-2.92384	-0.82102	-0.36157
H	-3.84192	-1.20103	-0.80923
C	2.49158	-0.30754	-0.83026
C	1.88674	-1.55523	-0.50626
C	1.57287	-1.55992	0.88475
C	1.98509	-0.29551	1.42206
C	2.54125	0.47638	0.36447
H	-1.32846	2.78690	-0.38545
H	0.77888	3.21006	-0.38138
H	-1.71704	-0.41976	-2.56445
H	-1.60694	1.56151	2.02697
H	-1.10988	-0.43168	2.68805
H	1.89651	0.01643	2.45691
H	2.94293	1.47971	0.45218
H	2.84651	-0.00444	-1.80826
H	1.69860	-2.36633	-1.20120
H	1.13747	-2.38076	1.44249
H	-1.25226	-2.28813	-1.59978

C

$G°_{solv}$ -968523.6002246

Ru	-0.57407	-0.02077	-0.03371
P	1.07404	-0.53614	1.48932
P	0.79772	-1.22503	-1.41789
P	0.57816	1.86008	-0.60210
C	2.21584	-1.95412	-0.51851
H	2.92390	-2.59734	-1.04124
C	2.35843	-1.61368	0.76212
H	3.19327	-1.95847	1.37259
C	-2.43574	0.97463	0.71775
C	-2.28840	-0.27121	1.39181
C	-2.35968	-1.32454	0.43093
C	-2.54214	-0.71600	-0.85198
C	-2.59676	0.69549	-0.68089
H	1.11099	1.92665	-1.91553
H	-0.25171	3.02079	-0.62709
H	1.77148	0.38397	2.29086
H	1.45366	-0.60023	-2.50932
H	0.26403	-2.34010	-2.10771
H	-2.63244	-1.24257	-1.79612
H	-2.75212	1.42835	-1.46477
H	-2.44751	1.95480	1.18084
H	-2.14160	-0.39693	2.45950
H	-2.31601	-2.38733	0.63781
H	0.59246	-1.38788	2.52291
O	2.64783	1.20793	0.06069

O	1.80623	2.40246	0.30598

$TS_{C,D}$

$G°_{solv}$ -968553.1942865

Ru	-0.61294	-0.03889	-0.00519
P	0.84512	-1.08516	-1.44512
P	0.95636	-0.68120	1.54308
P	0.65461	1.85500	-0.42818
O	2.58934	0.56748	0.03052
O	1.98615	2.25133	0.34287
C	2.49166	-1.22272	0.71189
H	3.38907	-1.42471	1.29440
C	2.43306	-1.46778	-0.62974
H	3.29660	-1.81027	-1.19626
C	-2.47016	-1.31624	0.21126
C	-2.54243	-0.57644	-1.01182
C	-2.55717	0.81315	-0.70199
C	-2.42488	-0.36765	1.27672
C	-2.48177	0.94562	0.72549
H	-0.13321	3.04018	-0.33377
H	0.98988	1.95009	-1.81219
H	1.28740	-0.40252	-2.60643
H	0.46754	-2.30640	-2.05755
H	0.61350	-1.76080	2.39964
H	1.48028	0.20041	2.51224
H	-2.47833	-2.39521	0.31065
H	-2.59042	-1.00219	-2.00837
H	-2.63426	1.62569	-1.41613
H	-2.49434	1.87470	1.28394
H	-2.35967	-0.60544	2.33338

D

$G°_{solv}$ -968622.5312716

R	-0.55991	-0.11643	-0.02583
P	1.02205	-1.11643	-1.32428
P	1.05655	-0.13484	1.58109
P	0.21146	1.95812	-0.71897
O	3.16412	0.08948	-0.14344
O	0.69507	2.99514	0.29455
C	2.68320	-0.72444	0.91901
H	3.44543	-1.09173	1.60940
C	2.66398	-1.20310	-0.46495
H	3.41115	-1.92479	-0.80178
C	-2.60325	-0.02707	-0.94464
C	-2.32473	-1.39300	-0.61990
C	-2.17887	-1.50959	0.78842
C	-2.34058	-0.19659	1.34301
C	-2.62066	0.70972	0.28296
H	-0.84494	2.51447	-1.51383
H	1.17136	1.83749	-1.77876
H	1.44982	-0.56729	-2.56135
H	0.86676	-2.46341	-1.72943
H	0.90689	-1.00440	2.68832
H	1.46982	1.03237	2.26427
H	-1.98801	-2.42088	1.34315
H	-2.24424	-2.20563	-1.33456
H	-2.80698	0.36842	-1.93320
H	-2.81084	1.77251	0.38882
H	-2.28923	0.06023	2.39555

Full Gaussian09 Reference. Gaussian 09, Revision B.01, M. J. Frisch, G. W. Trucks, H. B. Schlegel, G. E. Scuseria, M. A. Robb, J. R. Cheeseman, G. Scalmani, V. Barone, B. Mennucci, G. A. Petersson, H. Nakatsuji, M. Caricato, X. Li, H. P. Hratchian, A. F. Izmaylov, J. Bloino, G. Zheng, J. L. Sonnenberg, M. Hada, M. Ehara, K. Toyota, R. Fukuda, J. Hasegawa, M. Ishida, T. Nakajima, Y. Honda, O. Kitao, H. Nakai, T. Vreven, J. A. Montgomery, Jr., J. E. Peralta, F. Ogliaro, M. Bearpark, J. J. Heyd, E. Brothers, K. N. Kudin, V. N. Staroverov, R. Kobayashi, J. Normand, K. Raghavachari, A. Rendell, J. C. Burant, S. S. Iyengar, J. Tomasi, M. Cossi, N. Rega, J. M. Millam, M. Klene, J. E. Knox, J. B. Cross, V. Bakken, C. Adamo, J. Jaramillo, R. Gomperts, R. E. Stratmann, O. Yazyev, A. J. Austin, R. Cammi, C. Pomelli, J. W. Ochterski, R. L. Martin, K. Morokuma, V. G. Zakrzewski, G. A. Voth, P. Salvador, J. J. Dannenberg, S. Dapprich, A. D. Daniels, Ö. Farkas, J. B. Foresman, J. V. Ortiz, J. Cioslowski, and D. J. Fox, Gaussian, Inc., Wallingford CT, 2010.